JOURNAL OF VIROLOGY, May 2001, p. 4843–4853 Vol. 75, No. 10
0022-538X/01/$04.00+0 DOI: 10.1128/JVI.75.10.4843–4853.2001

Transcription Program of Human Herpesvirus 8 (Kaposi's Sarcoma-Associated Herpesvirus)

MINI PAULOSE-MURPHY,[1] NGUYEN-KHOI HA,[1] CHUNSHENG XIANG,[1] YIDONG CHEN,[2] LAURA GILLIM,[1] ROBERT YARCHOAN,[1] PAUL MELTZER,[2] MICHAEL BITTNER,[2] JEFFREY TRENT,[2] AND STEVEN ZEICHNER[1]*

HIV and AIDS Malignancy Branch, National Cancer Institute,[1] and Cancer Genetics Branch, National Human Genome Research Institute,[2] National Institutes of Health, Bethesda, Maryland 20892

Received 15 November 2000/Accepted 16 February 2001

Human herpesvirus 8 (HHV-8), a gammaherpesvirus implicated in Kaposi's sarcoma, primary effusion lymphoma, and Castleman's disease, encodes several pathogenically important cellular homologs. To define the HHV-8 transcription program, RNA obtained from latently infected body cavity-based lymphoma 1 cells induced to undergo lytic replication was used to query a custom HHV-8 DNA microarray containing nearly every known viral open reading frame. The patterns of viral gene expression offer insights into the replication and pathogenic strategies of HHV-8.

Human herpesvirus 8 (HHV-8) or Kaposi's sarcoma (KS)-associated herpesvirus (KSHV) was initially identified in KS lesions using representational difference analysis (8). Subsequent epidemiologic studies have implicated HHV-8 in all forms of KS (45) including classical KS, KS in AIDS patients and other immunosuppressed patients, and the endemic KS seen in human immunodeficiency virus (HIV)-negative patients in Africa. HHV-8 has also been correlated with body cavity-based lymphomas (6) and multicentric Castleman's disease (37).

HHV-8, a member of the lymphotropic (gamma) subclass of herpesviruses, has the greatest homologies to Epstein-Barr virus and herpesvirus saimiri (32). Analysis of the HHV-8 genome reveals a number of conserved sequences, as would be expected in any herpesvirus, including those which encode virion structural proteins and viral DNA polymerase (32). HHV-8 also encodes several protein homologs of host proteins, including interleukin-6 (IL-6), a G-protein-coupled receptor, chemokine-like molecules (vMIP-I, vMIP-II, and vMIP-III), interferon regulatory factor 1 (IRF-1), a complement binding protein, Bcl-2, and cyclin D (23, 26). These viral proteins potentially contribute to pathogenesis by optimizing the cellular environment for viral replication or modifying the host immune response. Like most herpesviruses, HHV-8 replicates using a strictly ordered program of gene expression (31, 43). The temporal regulation of gene expression is important for fully pathogenic infection. Identifying the times at which viral genes are expressed may provide insights into HHV-8 pathogenesis.

Presently, there are no highly efficient in vitro exogenous infection model systems for HHV-8 infection. However, body cavity-based lymphoma 1 (BCBL-1) cells latently infected with HHV-8 (29) provide an available approach to study the HHV-8 lytic cycle. Induction of BCBL-1 cells with phorbol esters such as 12-*O*-tetradecanoylphorbol-13-acetate (TPA) can initiate lytic replication of HHV-8. Studies using this cell line show that a significant number of HHV-8 genes are expressed following TPA treatment while only a small subset of these viral genes are expressed in the absence of induction (29). The elevated levels of viral transcripts are accompanied by an increased production of viral DNA (29). This system thus provides a means to study the program of HHV-8 gene expression and replication in a relatively homogeneous population of cells.

To better understand how the temporal pattern of HHV-8 gene expression contributes to viral replication and pathogenesis, we investigated the transcription program of HHV-8 genes using recently developed microarray technology (34). A custom HHV-8 microarray was constructed containing PCR-amplified fragments corresponding to each HHV-8 open reading frame (ORF) and used as hybridization targets for probes made from BCBL-1 cells induced to produce HHV-8 with TPA at serial times following induction. We compiled a comprehensive catalog of the viral genes differentially expressed during HHV-8 lytic infection. The identification of the expression pattern of viral genes during the viral replication cycle provides clues to understanding the HHV-8 replication strategies.

MATERIALS AND METHODS

Cell lines. BCBL-1 cells (29) (National Institutes of Health [NIH] AIDS Research and Reagent Program, Rockville, Md.) were cultured in RPMI 1640 (BioWhittaker, Walkersville, Md.) containing 10% inactivated fetal bovine serum (HyClone, Logan, Utah), 2 mM L-glutamine (Life Technologies Inc. [LTI], Gaithersburg, Md.), 100 U of penicillin (LTI)/ml, 100 μg of streptomycin (LTI)/ml, and 5.0×10^{-5} M 2-mercaptoethanol (Sigma Co., St. Louis, Mo.) (BCBL-1 medium) at 37°C with 5% CO_2. Cells were maintained at densities between 2.5×10^5 and 3.0×10^5 cells/ml and split every 3 to 4 days. Cells were seeded the day prior to induction at a density of $\sim 2.5 \times 10^5$ cells/ml and chemically induced into lytic cycle (29) with 20 ng of TPA (Sigma) per ml. One hour after TPA induction, cells were washed with BCBL-1 medium, fresh medium was added, and cells were incubated at 37°C.

Construction of HHV-8 microarrays. Microarray detectors for nearly all the known HHV-8 ORFs and expressed message were constructed based on the published HHV-8 sequence (32). The viral array elements include sequences for

* Corresponding author. Mailing address: NIH, NCI, Bldg. 10, Room 10S255, MSC 1868, Bethesda, MD 20892-1868. Phone: (301) 402-3637. Fax: (301) 480-8250. E-mail: zeichner@nih.gov.

82 HHV-8 ORFs, latency-associated transcripts T0.7 and T1.1, and two additional fragments from the HHV-8 genome between bases 90541 and 89600 and bases 90173 and 90643. HHV-8 ORF 58 was not included on the array due to insufficient PCR product. ORFs K8, K8.1, and K8.2 were also excluded because we were unable to produce PCR products that effectively delineated these alternatively spliced ORFs from ORF 50. The viral array elements were supplemented with a subset of 88 cellular genes that were used for internal hybridization and normalization controls. These genes are preselected by the National Human Genome Research Institute, NIH (Bethesda, Md.), and have been observed to have relatively invariant expression under many conditions (18). For example, included in this set of cellular genes are glyceraldehyde-3-phosphate dehydrogenase, cytoplasmic beta-actin, human superoxide dismutase, and human malate dehydrogenase. Primers (Sigma Genosys, The Woodlands, Tex.; BioServ Technologies, Laurel, Md.) were designed (Table 1) to amplify fragments between 200 and 1,000 bases long from each viral ORF. Fragments were amplified using BCBL-1 high-molecular-weight DNA as a template. All products showed a single band of appropriate size by agarose gel electrophoresis. Following PCR, the product was ethanol precipitated, washed twice with 70% ethanol, and then resuspended in Tris-EDTA buffer. Microarrays were prepared by robotically spotting individual DNA species (PCR product concentration of approximately 0.5 mg/ml) on poly-L-lysine-coated glass slides as previously described (13, 36).

RNA preparation. TPA-treated and untreated BCBL-1 cells were collected 0, 3, 4, 8, 10, 12, 24, 36, 48, 72, and 96 h postinduction (hpi). Poly(A)$^+$ RNA was isolated using the Fast Track 2.0 kit (Invitrogen, Carlsbad, Calif.) following the manufacturer's instructions.

DNA microarray analysis. Poly(A)$^+$ RNA isolated from untreated control BCBL-1 cells and TPA-treated BCBL-1 cells was reverse transcribed using an oligo(dT) primer (LTI) and labeled with Cy3- and Cy5-dUTP (Amersham Pharmacia), respectively. The paired reactions were combined, and unincorporated fluor-dUTPs were removed with Microcon 30 filtration spin columns (Amicon, Millipore Corp., Bedford, Mass.). Purified fluorescently labeled probe was mixed with Cot-1 DNA (Boehringer Mannheim, Indianapolis, Ind.), poly(A) (LTI), and yeast tRNA (Sigma) and then applied to the microarray for hybridization at 65°C for 16 to 18 h. Following hybridization, slides were washed in 1× SSC (1× SSC is 0.15 M NaCl plus 0.015 M sodium citrate) for 1 min, followed by washes in 0.2× SSC and 0.05× SSC for 1 min and 20 s, respectively. Hybridizations were repeated with duplicate arrays and additionally performed with independent RNA preparations. For selected time points, the arrays were also queried with probes produced via reverse labeling, that is, TPA-treated cell RNA was labeled using Cy3-dUTP instead of Cy5-dUTP and the untreated cell RNA was labeled using Cy5-dUTP instead of Cy3-dUTP. The data obtained using the different arrays and experiments were consistent.

Slides were scanned with the Axon GenePix 4000 scanner (Axon Instruments, Inc., Foster City, Calif.) and analyzed using the ArraySuite program, developed by Chen et al. (4, 9), based on the IP Lab Spectrum software. In the experiment displayed here, which is representative of one array experiment, the TPA-treated image (Cy5 labeled) was assigned a red color and the untreated control image (Cy3 labeled) was assigned a green color to form a pseudocolored image. Intensity data were integrated over 225-μm-square pixels and recorded at 16 bits. The final reported probe intensity for every spot was the average fluorescent intensity for the spot minus the local background intensity. The ratios of emission fluorescence for all targets were determined by taking the final reported probe intensity at each spot in the TPA-treated image and dividing by the final probe intensity of the same spot in the untreated control hybridization. A normalization factor, based on the distribution of ratios for the 88 cellular genes, was applied to ratios from the viral targets, and calibrated ratios were reported (4, 9). Normalization ensures that the obtained ratios are not affected by differential labeling or hybridization efficiency. For normalization, the average intensity, in both Cy3 and Cy5 channels, for the 88 cellular genes was determined (18). The ratio variance of these 88 cellular genes is also used to calculate 99% confidence intervals where the ratios are considered to be no different from 1. Calibrated expression ratios for each gene were cataloged based on a hierarchical clustering program (average-linkage algorithm) (14). To visualize the temporal trend of each ORF, we normalized the log-transformed gene expression ratio by its mean and standard deviation, or $z_{ij} = (\log t_{ij} - \mu_i)/\sigma_i$, where z_{ij} is the normalized log-transformed expression ratio, t_{ij} is the expression ratio for i^{th} ORF at j^{th} time point, and μ_i and σ_i are the mean and standard deviation of the log ratio of i^{th} ORF across all time points, respectively.

Northern blot analysis. One microgram of poly(A)$^+$ RNA was fractionated on a 1% agarose-formaldehyde gel and transferred to a nylon membrane (Nytran; Schleicher and Schuell, Keene, N.H.) by standard procedures (3). DNA probes were labeled with [α-^{32}P]dCTP (3,000 Ci/mmol) (Amersham Pharmacia) by the random-primed method using the Rediprime II labeling kit (Amersham Pharmacia). The DNA probes used in the hybridization reactions were PCR-amplified products of the HHV-8 ORFs. Blots were prehybridized for 1 h and hybridized for 2 h at 68°C in ExpressHyb solution (Clontech, Palo Alto, Calif.). Filters were washed in buffer A (2× SSC and 0.05% sodium dodecyl sulfate [SDS]) three times for 5 min each and then three times for 15 min each at room temperature, followed by two washes in buffer B (0.1× SSC and 0.1% SDS) for 20 min each at 50°C. The washed blots were placed on film at −80°C. For quantitation of RNA loading, blots were stripped by boiling in 0.5% SDS for 15 min and reprobed with glyceraldehyde-3-phosphate dehydrogenase.

RESULTS

HHV-8 transcription program. To identify changes in gene expression during the HHV-8 lytic replication cycle, we fabricated custom viral microarrays containing nearly all the known HHV-8 ORFs, based on published HHV-8 sequence data (32). The 88 viral array elements were supplemented with 88 cellular genes. Poly(A)$^+$ RNA was isolated from TPA-treated BCBL-1 cells at 0, 3, 8, 10, 12, 24, 36, 48, 72, and 96 hpi to encompass the complete lytic cycle (29, 33). RNA from induced and control, uninduced BCBL-1 cells at corresponding time points was reverse transcribed into fluorescently labeled cDNA in the presence of Cy3- or Cy5-dUTP. The labeled cDNAs were hybridized to the custom HHV-8 microarray. The arrays were scanned for fluorescence intensities in each spot with a confocal laser array scanner, and images were constructed using a pseudocolor scheme, with spots corresponding to genes highly expressed during HHV-8 replication appearing red (Fig. 1). The array consists of four subarrays, each containing 22 HHV-8 elements (V regions) and 22 control cellular genes (C regions). The time (hours) after TPA induction is indicated at the right. Examination of the pseudocolored composite array image shows that, during infection, different viral genes can be seen to increase (red spots) and decrease (green to light-green spots) in expression in a distinct temporal pattern while cellular genes remain unchanged (yellow-green spots), as would be expected. Even at this relatively gross, qualitative level, a temporally controlled viral transcription program is apparent, with some viral spots becoming red early after induction and others turning red later. Occasional white spots indicate saturation (maximal expression).

Quantitative information extracted from the arrays is presented in Table 2. The data are normalized to the maximal expression for each gene and then color coded according to the time of peak expression. Noting the time at which expression reaches a peak emphasizes the period of maximal expression and also shows the relative patterns of increased and decreased gene expression. For example, ORF 37, which initially increases in expression at 10 hpi, shows peak expression levels at 36 hpi and then displays a gradual decline in gene expression, whereas ORF 16, which also increases in expression at 10 hpi, does not show maximal expression until 48 hpi but shows a much faster decline. Of the 88 viral elements on the HHV-8 array, 1% were at maximum expression at 12 hpi, 17% were at maximum expression at 24 hpi, 54% were at maximum expression at 36 hpi, 26% were at maximum expression at 48 hpi, 1% were at maximum expression at 72 hpi, and 1% were at maximum expression at 96 hpi. Table 1 also displays the times (hours postinduction) at which a doubling in expression (DT) is seen for each gene compared to baseline expression (0 hpi). The DT emphasizes the time at which gene expression first

TABLE 1. HHV-8 primers

ORF	Forward primer (5′)	Reverse primer (3′)
90541–89600	TGAACGCAATCTGAGCTTGATG	AGTCGATGATGGTGCTGGACTG
90173–90643	AGTCCAGCACCATCATCGACTTC	TCCCAGAGGATGTTATCGCAAC
ORF K1	GCATCCTTGCCAATATCCTGG	CCAATCCACTGGTTGCGTATAGTC
ORF K2	GGGATAGAGTCCAAAACACGCAC	TCGGTTCACTGCTGGTATCTGG
ORF K3	CGCCCAAGTTGTTACAGTCACACC	GATGTTCCTGTCTGCTGGATTTG
ORF K4.2	CCTCGCTTGGTCAGCAAAATAAC	ACTGCTTGCCACGTTTTACCTG
ORF K5	CGTCACGTTCTTTGTCTCCAGAGG	TATGTAGGGAAGAGGTGGGGAAC
ORF K6	TGCTGCATCAGCTTCTTCACC	GACCATTACCACAGGTGCTTCTG
ORF K7	GCTTGAGTCAGTTTAGCACTGGGAC	TGGCAAGGTTTTTGGGCAAATC
ORF K9	TGGTAACGGTGAATTTGCCAAC	ATGAACCATCCAGGTCGGAGTCAC
ORF K10	CCTTGAAGGTTCGAGAGCGTAAG	TATACGGGGATTCCTAGCAGCC
ORF K11	CCAACAAAGTATGCTGGGTATTCC	ATTGCCTACCGATGGTGGATC
ORF K12	TGCAACTCGTGTCCTGAATGCTAC	TGGATAGAGGCTTAACGGTGTTTG
ORF K13	GTGTAAGAATGTCTGTGGTGTGCTG	ACGGATGACAGGGAAGTGGTATTG
ORF K14	CGTAGTGGAGGGCGGAGTTATATC	GTGAACTGCTCCTGGGTAGAAGAG
ORF K15	GCAAACACACATGCAGCGAG	AGCCATTCTATCACTTGGTGGAAC
ORF 2	CATGCGAGAGAAACACGTCACAC	CGGTTGATACCAAACTCGGGATC
ORF 4	AAGTCCTGTCCAAACCCAGGTG	GCGTGGCTTAGTGGAACTCTTG
ORF 6	TCGATGCAACCACAGCTTCTG	GTAAGATGACCCATCCAGTGCAG
ORF 7	CTAGAATGCCTTCAGGAAGTGTGTC	TGTTAGGTACAGCCCCGTTGTG
ORF 8	GAGCTTTTTCGGTTCAACCTGG	ACCATGCCCTGGAGAGTTCTTC
ORF 9	CAATGCTCCTATGTCGCACCTC	TCAACATGGGTCTGAAACCGTAG
ORF 10	ATTTTTTGTCAGTCCCCTGCCCCC	TCGTAGAAGCTGTATGGTGCCTG
ORF 11	CGTCATCTCTAATCGAGTACCCCTC	GATGGCTGTGACTTTGCATGG
ORF 16	CGAACCTGAGTACCTGTACCATCC	TGTCATTCTCCGTCCCCTTCTTC
ORF 17	TAGAGCGACTGCTGGCTTCAAC	CGAGTGGGTGGTTTCCAGATTC
ORF 18	GGAAAATACGTGTGTGAGACCGAG	TGTTGTTAAACGCACCAAGGTAGG
ORF 19	GCAGTGTGGGGATTATGTAGTGCTC	GGCTTGTTCAGGTCCATGACTCAC
ORF 20	TCGTTCTCGATTTCGCACGAG	TGGAGGTGCTTGATTCGTCGTC
ORF 21	ACGACGAATCAAGCACCTCCAC	ACGTTCCAGGGCTGCATCATTC
ORF 22	CAACGGCGACGACAATAACC	CGAGATGCGGCGGAGAAAATAC
ORF 23	CACATATCAGTTCGACCACCCC	AATCCTGAAGTCCCGATGCCACTG
ORF 24	CCTGAGAAACGAACAGCATTCC	CCCGTCTGCACGTAAAAATCC
ORF 25	GGACCTGCGGAGAATGATAGATG	ATTAACCACCCACGTCTCGGTC
ORF 26	CCGAAAGGATTCCACCATTGTG	TGATGTCATCTGGGACGCTCAAC
ORF 27	ACGCCATCAAAGACGCCTTC	GAATCAAGGGAGGGGTGGATAG
ORF 28	TGTTCCTGGCGGCTCGACTG	TGGCATGTATATTGTACGGTAGGG
ORF 29a	CTACGTGCTTTTGGTGGGCTAC	TGGAAACATACTGCACACGGCAC
ORF 29b	CCATGACAACTGCCACAAGTAAGTC	TCAGGAACGCCCAGGAAAAG
ORF 30	GTGGTGAATGAGAAAGATTTTGAGG	AGGTCCATCAGCAGGCAGAGTC
ORF 31	AAAGACTCTGCCTGCTGATGGAC	ATTTTGTCCGCACCCGCTTG
ORF 32	GGAGGAAAACCAACTTGCGTCTTC	TGGCAGCTCTTATCCAGGCACTAG
ORF 33	CCAATGTCAGGGGACCATATCAAG	ACAATGGGATCGAACAGAAGACC
ORF 34	CACTTGCCTAGACTGGAGAAGCTC	CGATGGGATGATTAGATAGTCGCC
ORF 35	GCTATTTGATCGTTTTGGGGGTAG	TTAGGGAGTTTCAGGGCACACC
ORF 36	TCACTCCTCTTCGGAGATCAAGG	AGCACTGCTTCTGAAACGCCAG
ORF 37	AAGACTATCTGGTTGACACCCTGG	CGATTAGCAGCGTAGGAATCTCCAC
ORF 38	CTCCTATCTATCTGCAAACGTCCC	TGCTCAAGCAACATGCCCTTTTC
ORF 39	CGTTTCGTCGATTTCACTGTCAC	TTCCCCTGCTACTTCAACAATCTG
ORF 40	ACGTCCACTGCCGCATTATTG	AGTTGTATCTAAGCTCCACGCTCC
ORF 41	CAACCTCGATGGGATATTTCCTC	TCATTTCCTTTGCGTCTTGGG
ORF 42	TCCAGGTGCTTGGTAAAGATGG	AAAACAACGCACTGGTTGGAAG
ORF 43	TGTTGGCGGTCAGCAGATTC	TCCCTCTTTGAGATCCTGCAAGG
ORF 44	GTTCATCCTCAACATGACATCGG	AAACACCTCACAGACCACTGGG
ORF 45	GTTGTGCTTCCTGATGAAATCGAG	CATATTCCCACCTCCACCTCTTTC
ORF 46	GCGAGTCAAATAGTCGTTGGCTAG	TGGCACCTAAGTGGATTTCCTTTC
ORF 47	TGCTGCTTTTAGCCCGAGTCTG	TGGTCACATCTCACGCATACGTC
ORF 48	TCACACGTCTGGCTGAGATTTTC	TTCGTCAAGACCGAGCGTATTC
ORF 49	TGCGTGTTTACAATGGTGTAGGTG	TTTAGGTATCATTACCCGTCCTGG
ORF 50	TTTTTCGTGCCTCTCGAATGAG	TCCACCAGAAGGTGACGGTATATC
ORF 52	TATTGGCACCAGGAGGCGGTTTAG	CCCAAAAAGGACCTTACGATGGAAG
ORF 53	GACCACCTCGTCCACAAACTTG	CGATACTAGGTCACTGCTGGGTTAC
ORF 54	CGAGAGCAAATGAAGCCAGACTC	CTTCGTGGGTATGTTTTCGGAC
ORF 55	GCGTGAGAGGCAATACAGAAGTG	CCTGGACGTGTTGCGGTATAAAC
ORF 56	ATCGACCGCACCATAGACCAGATC	ACTTCGCTCACCCTAATGGAATG
ORF 57	CAATGTCTTCATTCCCGCCC	TCACTGTTTCTGCACAAGCTGTG
ORF 59	TCGGGAACCTTTTGCGAAG	TGCCTGTGGATTTTCACTATGGG
ORF 60	TGGGTTTTTCCTGTATCTCCACC	CTTGGCAGAACCGATGGTTTC

Continued on following page

TABLE 1—*Continued*

ORF	Forward primer (5′)	Reverse primer (3′)
ORF 61	ATGCAGGCGTTGATGACGAG	TTTCTAAAGGTTAGGGTCGGGTG
ORF 62	AGGTGGTGGCGGAAAATACTCC	GGGTATATTGGCTTTGCGATTG
ORF 63	TCGGACATTCCACTGCGTTG	GGGTATATTGGCTTTGCGATTG
ORF 64	AACAAGACCACAAGCACGGATG	TCGGAGGATACCAGGTTTTGG
ORF 65	TGAGAGGGTTGTGAGAATGTCTGAC	TGGTGGCTCGCATGAATACC
ORF 66	ACGTTGGTGGGAGGAAAATTG	TCTTGGTTTGGTTTGGATGAGG
ORF 67	CCTCATCCAAACCAAACCAAGAC	TTTATGCTAAGGGCGGTGCTAC
ORF 68	TCAACTCACGATCCAGGGAAAC	GACACCACCTTAGCATTGAGGG
ORF 69	AACAGTAATGCTGCCCCTAGACC	AATGTCATCCCGCATCTCGTC
ORF 70	ATACGAATGGTAGGATGCGGG	TCGATTCAGCATGAGGTAACTGGG
ORF 72	GGTATCCTGCGGAATGACGTTG	TGCGTAAGTTACTGGGCACATG
ORF 73	GGTCATTGCCCCAAAAAATCAC	GCATCCAAAGTTCACAACAGCAG
ORF 74	AAGTGAGCGTGTGTGAGATGACC	GAGACCGTACATCCTCTGCCTAAAG
ORF 75	GTTAGGTCTGGTGGAACATGCTG	TCATTGTATCTGGGCACGACATAGG
T0.7	CGGTGTTTGTGGCAGTTCATGTC	TGGCACACGCTGCAATGTACTG
T1.1	GGATTTTGTGCTCGCTGCTTG	GGATAAAAACCTTGCCGTCTGGTC

starts to increase substantially (by at least twofold) over baseline and hence gives a sense of when the expression of a particular gene commences. Peak times and DTs may not necessarily be consistent, since peak times reflect RNA accumulation, not just RNA production, and are thus influenced by such posttranscriptional factors as RNA stability. It should be noted that the results obtained from the arrays are, strictly, only a measure of RNA quantity and hence are an indirect indication of instantaneous transcriptional activity. The DTs enable the genes to be grouped based on the time of the onset of expression. Relationships can be seen between patterns in the onset and peak levels of gene expression and gene function at particular stages of the viral lytic cycle.

Analysis of the DTs reveals a pattern of differential viral gene expression in which increased expression of certain viral transcripts is detected much earlier than is increased expression of others. The earliest transcriptionally active genes showing one of the first DTs are ORFs 57, K4.2, and K5, which encode immediate-early proteins involved in viral gene regulation. These genes show increased expression as early as 8 hpi. Following the expression of these immediate-early proteins, ORF 50, which encodes a replication and transcription activa-

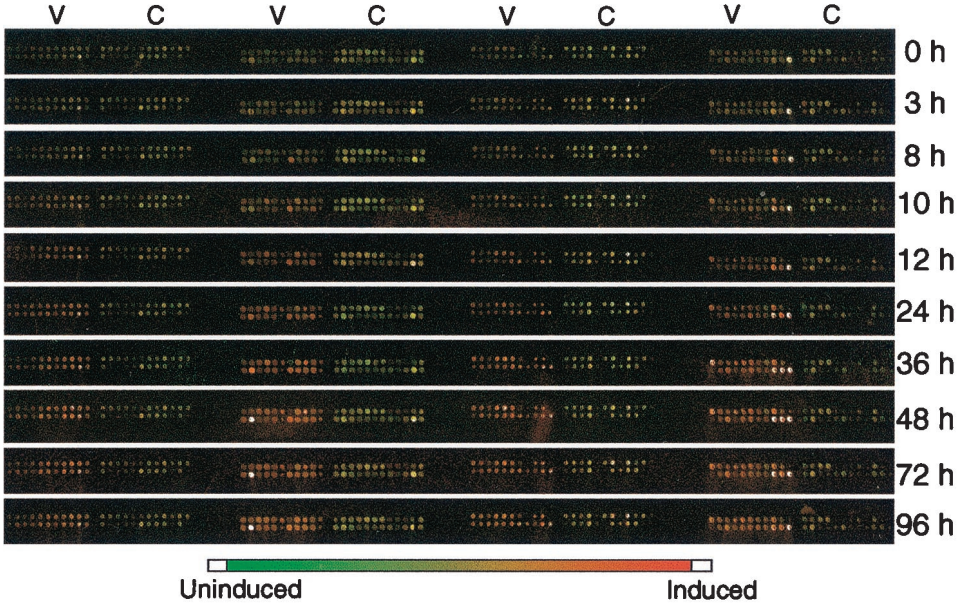

FIG. 1. Microarray images from BCBL-1 cells induced with TPA. Poly(A)$^+$ RNA was isolated from TPA-induced and uninduced BCBL-1 cells at 0, 3, 8, 10, 12, 24, 36, 48, 72, and 96 h after induction. Poly(A)$^+$ RNA was reverse transcribed into fluorescently labeled cDNA in the presence of Cy3-dUTP (uninduced; pseudocolored green) or Cy5-dUTP (induced; pseudocolored red). The labeled cDNAs were hybridized to an HHV-8 array containing viral ORFs and expressed messages (V regions), as well as a subset of cellular genes (C regions). The arrays were scanned, and pseudocolor images were constructed. The intensities of gene expression are depicted on the color scale below the image. Down-regulated spots appear dark green, greenish-yellow spots indicate no change in expression between untreated and treated samples, and spots corresponding to genes overexpressed during HHV-8 replication appear red. White spots indicate maximal gene expression intensity (saturation) in the Cy5 channel (635 nm), which indicates very high expression of that particular viral gene.

TABLE 2. HHV-8 genes on array and their expression during the lytic replication cycle[a]

ORF	Putative Function	DT	Calibrated Ratio										Normalized Data									
			0h	3h	8h	10h	12h	24h	36h	48h	72h	96h	0h	3h	8h	10h	12h	24h	36h	48h	72h	96h
ORF K1	Membrane protein	10	1.1	1.3	1.4	2.2	2.1	3.0	6.2	5.9	3.8	3.0	18	21	23	36	34	48	100	94	60	48
ORF 4	Complement binding protein	24	1.3	1.1	1.3	2.2	1.6	3.5	4.5	5.3	5.1	3.9	24	21	24	41	31	65	84	100	96	72
ORF 6	DNA binding protein	10	0.9	0.9	1.0	3.9	7.1	4.4	5.4	2.7	2.6	4.4	12	12	14	55	100	62	75	38	37	62
ORF 7	Transport protein	10	1.1	1.3	1.0	2.9	1.5	2.3	3.7	3.1	2.4	2.4	31	34	28	79	41	62	100	84	64	66
ORF 8	Glycoprotein B	10	0.9	0.7	1.0	3.4	3.6	4.4	2.0	2.2	1.1	1.7	21	16	23	77	81	100	44	50	24	39
ORF 9	DNA polymerase	10	0.9	0.9	1.0	3.1	3.9	5.7	2.4	2.4	1.5	3.0	15	16	18	54	68	100	42	43	27	52
ORF 10		12	1.5	1.3	1.8	2.9	4.5	4.6	9.7	4.7	3.6	3.2	15	13	18	30	46	48	100	49	37	33
ORF 11		10	1.6	1.4	2.8	3.7	4.7	9.3	15.0	13.8	5.9	4.3	11	9	19	24	31	62	100	92	39	29
ORF K2	vIL-6	8	1.4	2.0	5.9	5.9	7.4	14.7	12.3	10.6	5.4	6.9	9	14	40	40	50	100	84	72	36	47
ORF 2	DHFR	10	1.0	0.9	1.4	3.4	3.3	5.5	5.1	3.7	3.8	2.5	18	16	25	61	59	100	92	67	68	45
ORF K3	IE-1	10	1.0	0.8	1.8	2.9	4.8	7.4	9.9	12.0	5.7	4.6	9	7	15	24	40	62	83	100	47	38
ORF 70	Thymidylate synthase	10	0.9	0.8	1.3	3.0	4.1	3.2	4.6	4.5	2.5	4.3	20	18	29	67	90	70	100	98	55	94
ORF K4.2	IE-3	8	1.4	1.3	4.4	5.6	8.0	9.5	10.4	10.8	5.5	5.9	13	12	41	51	74	88	96	100	51	54
ORF K5	BHV4-IE1 homolog	8	1.1	1.3	3.3	4.1	4.4	8.5	10.5	10.2	4.8	4.4	11	13	31	39	41	81	100	97	45	42
ORF K6	vMIP-IA	12	1.2	1.0	1.5	2.3	3.1	7.6	13.6	14.1	7.3	4.8	8	7	11	16	22	54	96	100	52	34
ORF K7		24	1.2	1.0	1.3	1.5	1.6	4.5	7.8	5.4	4.1	3.0	16	13	17	19	20	57	100	69	52	39
ORF 16	vBcl-2	10	1.0	0.9	1.2	2.0	1.9	5.2	6.2	7.5	4.4	2.4	14	12	16	26	26	69	83	100	59	31
ORF 17	Minor capsid protein	24	1.7	1.1	1.3	1.3	1.4	7.5	12.9	6.5	7.5	4.5	13	8	10	10	11	59	100	51	59	35
ORF 18		24	1.5	1.3	1.4	1.7	1.5	4.0	10.2	8.5	4.9	3.4	14	13	14	17	15	39	100	84	48	34
ORF 19	Tegument protein	24	1.1	1.1	1.8	2.0	1.6	4.5	8.1	4.7	3.9	3.7	14	13	22	24	20	56	100	58	48	46
ORF 20	Fusion protein	24	0.9	0.9	1.0	1.9	1.7	3.7	2.1	2.0	1.8	2.2	25	23	27	51	48	100	57	55	50	61
ORF 21	Thymidine kinase	10	0.9	1.0	0.9	1.9	1.3	3.9	4.3	2.6	3.6	3.8	22	23	21	45	30	91	100	61	84	89
ORF 22	Glycoprotein H	24	1.0	1.1	1.0	1.7	1.3	3.9	7.7	4.6	5.2	4.0	13	15	13	23	17	51	100	60	68	52
ORF 23		24	1.3	1.1	1.7	1.4	1.2	3.5	8.2	6.0	5.1	3.6	16	14	20	18	14	43	100	73	63	44
ORF 24		24	1.1	0.8	0.9	1.7	1.3	3.2	3.9	3.3	3.3	2.4	29	21	23	44	34	82	100	84	85	62
ORF 25	Major capsid protein	24	0.9	0.8	0.9	1.4	1.5	4.1	4.1	2.9	3.0	3.9	21	20	22	34	37	100	98	69	74	95
ORF 26	Minor capsid protein	24	1.4	1.0	1.4	1.5	1.2	4.8	6.3	2.8	5.0	3.9	22	15	21	23	19	75	100	45	78	61
ORF 27		24	1.8	1.5	2.1	2.1	1.8	6.6	10.2	5.6	6.4	4.5	18	14	21	20	18	64	100	55	63	44
ORF 28		24	1.1	0.8	0.8	2.0	1.5	3.6	0.9	2.1	1.8	2.0	31	22	23	55	43	100	26	60	51	56
ORF 29B	Packaging protein	24	1.0	0.8	1.4	1.9	1.6	3.1	3.8	4.5	2.3	3.3	22	18	31	42	36	71	85	100	52	75
ORF 30		24	1.8	1.2	2.3	2.4	2.1	4.7	7.7	5.8	4.8	3.6	24	16	29	31	28	61	100	75	62	46
ORF 31		10	1.1	0.9	1.1	2.4	2.1	3.3	2.6	1.9	2.2	3.1	35	28	35	75	64	100	80	58	68	94
ORF 32	Tegument protein	10	0.9	1.0	1.0	1.8	1.7	4.7	7.1	2.7	4.8	4.1	13	15	14	26	25	66	100	38	67	58
ORF 33		24	1.6	1.1	1.7	1.6	1.7	4.6	8.3	5.7	6.4	4.6	19	13	20	20	21	55	100	68	77	56
ORF 29A	Packaging protein	24	1.3	1.2	1.5	1.6	1.8	5.3	6.6	5.6	5.2	4.1	20	19	24	25	27	80	100	85	79	62
ORF 34		36	1.4	1.0	1.4	2.4	1.9	2.7	3.8	2.5	2.8	4.2	32	25	34	57	45	65	91	59	67	100
ORF 35		10	1.4	0.9	1.5	3.5	3.6	3.6	4.3	3.6	2.9	2.6	31	21	33	81	82	83	100	82	67	59
ORF 36	Protein kinase	10	0.9	0.9	1.4	4.0	4.7	7.5	8.4	4.1	4.2	4.1	11	10	17	47	55	89	100	48	50	48
ORF 37	Alkaline exonuclease	10	1.3	1.1	1.9	3.2	4.8	8.7	10.3	9.9	4.8	4.6	13	11	18	31	47	85	100	96	47	45
ORF 38	Tegument protein	12	1.6	1.3	2.8	3.0	4.2	7.1	10.7	9.7	5.9	5.2	15	12	26	28	39	66	100	91	55	48
ORF 39	Glycoprotein M	24	1.3	1.0	1.6	1.8	2.0	6.4	6.6	7.0	6.0	4.0	18	14	22	26	29	92	94	100	86	58
ORF 40	Helicase/Primase subunit	24	1.3	1.3	1.2	2.5	2.4	4.4	7.9	5.5	4.3	4.0	17	16	15	32	30	56	100	70	55	50
ORF 41	Helicase/Primase subunit	24	1.7	1.5	2.0	1.9	2.1	4.4	9.3	8.3	4.8	3.8	18	16	21	20	23	47	100	89	51	41
ORF 42		24	1.9	1.4	2.0	1.9	1.5	4.2	9.1	7.3	6.1	4.8	20	15	22	21	17	47	100	80	67	52
ORF 43	Minor Capsid Protein	24	1.3	1.1	1.4	2.0	1.4	4.2	2.4	4.1	4.7	3.0	29	23	30	44	30	90	51	87	100	64
ORF 44	Helicase/Primase subunit	24	1.1	1.3	1.1	1.8	1.6	3.8	4.6	4.2	3.6	3.5	23	28	24	39	34	83	100	91	78	75
ORF 45	Transactivator	12	1.4	1.3	1.7	2.2	4.2	8.5	10.9	10.1	5.5	4.9	13	12	16	20	38	78	100	92	50	44
ORF 46	Uracil DNA glucosidase	10	1.1	0.9	1.6	2.7	3.7	6.9	11.0	5.7	5.4	5.7	10	8	14	25	33	63	100	51	49	52
ORF 47	Glycoprotein L	10	1.1	0.9	1.5	3.1	3.9	6.8	6.3	4.3	3.6	4.0	16	13	22	46	58	100	93	63	54	59
ORF 48	Glycoprotein	24	1.1	1.0	0.9	1.7	1.4	4.5	7.8	7.5	7.0	5.1	14	13	11	21	18	58	100	96	90	66
ORF 49		10	1.4	1.3	2.3	3.5	6.0	10.5	9.6	11.6	4.2	5.3	12	11	20	30	52	90	83	100	36	46
ORF 50	Rta	10	1.1	1.1	2.0	4.3	5.2	10.7	9.6	6.9	3.8	5.4	10	10	19	40	49	100	90	64	36	50
ORF 52		24	1.5	1.1	1.6	2.1	2.6	5.9	8.3	9.8	8.3	5.1	16	11	16	22	27	60	84	100	85	52
ORF 53		24	1.3	1.1	1.3	1.8	1.8	5.3	9.1	9.6	8.3	5.6	13	12	13	18	18	55	94	100	86	58
ORF 54	dUTPase	24	1.9	1.6	2.2	2.6	2.8	4.3	9.1	9.6	5.3	4.6	20	17	23	27	29	45	95	100	55	48
ORF 55		24	1.5	1.2	1.6	2.5	2.5	5.0	11.9	10.6	6.4	4.8	12	10	14	21	21	42	100	89	54	40
ORF 56	DNA replication protein	10	1.1	1.0	1.5	2.6	3.3	4.5	5.1	3.3	4.1	3.1	23	19	30	52	64	88	100	64	80	62
ORF 57	Immediate early protein	8	1.3	1.4	5.2	5.9	7.5	7.9	9.6	11.2	4.8	5.0	12	12	46	53	67	71	86	100	43	45
ORF K9	vIRF-1	10	1.2	1.3	2.0	2.7	4.8	17.0	16.0	14.2	9.7	6.1	7	8	12	16	28	100	94	84	57	36
ORF K10		12	1.2	1.0	1.3	1.6	2.4	6.6	7.0	6.2	5.7	3.2	17	14	18	23	34	95	100	88	81	46
ORF K11		24	1.0	0.9	1.0	1.6	1.7	3.3	4.7	4.7	3.0	2.6	20	18	21	35	36	70	99.8	100	64	55
ORF 59	Processivity factor (PF-8)	10	0.8	0.8	0.9	2.6	5.4	7.0	7.8	4.1	4.8	5.8	10	11	12	33	69	90	100	53	61	75
ORF 60	Ribonucleotide reductase	10	0.8	0.8	1.0	3.1	4.5	5.4	5.6	3.1	2.6	4.5	14	14	18	56	81	97	100	56	47	82
ORF 61	Ribonucleotide reductase	10	0.8	0.6	1.0	3.1	4.2	6.2	4.2	6.7	2.2	3.0	12	8	14	47	63	93	62	100	32	45
ORF 62	Assembly/DNA Maturation	10	0.8	1.0	1.1	2.4	1.3	2.6	0.7	2.6	1.5	2.0	32	39	40	92	51	99	25	100	57	77
ORF 63	Tegument protein	10	0.9	1.2	0.9	2.4	1.9	2.7	3.7	2.5	1.5	2.0	25	32	26	65	50	74	100	69	41	55
ORF 64	Tegument protein	24	1.3	1.2	1.5	1.8	1.7	2.7	5.3	5.3	3.3	2.4	25	22	28	34	32	50	100	99	62	45
ORF 65	Minor capsid protein	24	1.4	0.9	1.4	1.4	1.9	7.4	8.2	10.0	9.6	3.1	14	9	14	14	19	74	82	100	97	31
ORF 66	Capsid protein	24	1.2	1.1	1.1	1.6	2.1	6.4	8.6	6.5	6.3	4.2	14	12	13	18	25	75	100	76	73	49
ORF 67	Tegument protein	12	0.9	1.0	0.9	1.6	1.8	5.1	4.9	4.1	5.0	3.5	18	21	18	32	36	100	97	81	97	69
ORF 68	Glycoprotein	12	1.1	1.0	0.9	1.3	1.8	3.7	7.2	4.7	2.1	3.7	15	14	12	19	25	52	100	66	29	52
ORF 69		24	1.3	0.9	1.1	1.8	2.3	5.6	7.9	9.3	4.0	2.8	14	9	12	19	24	60	85	100	43	30
ORF K12	Kaposin	24	1.2	1.3	1.4	1.2	1.5	5.4	10.4	11.2	10.0	4.2	11	11	13	11	13	48	93	100	89	37
ORF K13	vFLIP		1.4	1.8	2.0	1.7	1.9	2.1	3.6	3.3	1.6	1.8	39	48	56	47	51	57	100	91	43	49
ORF 72	vCyclin D		1.0	0.7	0.9	2.1	0.6	1.3	1.5	5.7	2.2	2.0	18	11	16	36	11	22	27	100	39	35
ORF 73	Latent associated antigen		1.2	1.5	1.4	1.5	1.5	1.3	1.8	1.3	0.9	1.7	65	82	79	83	83	74	100	73	49	93
ORF K14	vOX-2	10	0.8	0.7	1.3	2.6	3.4	5.8	5.4	4.7	2.8	3.5	14	12	23	44	58	100	92	80	48	60
ORF 74	vG-protein coupled receptor	12	1.3	1.1	2.0	2.7	3.7	5.8	7.6	9.6	3.9	3.3	14	11	21	28	38	61	80	100	40	34
ORF 75	Tegument protein, FGARAT	24	1.5	1.2	1.3	1.7	1.8	3.8	5.0	4.5	3.0	3.3	30	23	27	34	35	75	100	89	60	65
ORF K15	Membrane protein	24	1.0	1.0	1.1	1.8	1.7	4.0	4.0	3.8	3.2	2.8	26	24	27	45	42	100	99.5	94	80	70
T0.7	Latency associated transcript	24	1.3	1.3	1.5	1.1	1.4	5.8	11.9	7.9	7.2	4.0	11	11	13	9	11	48	100	66	61	33
T1.1	(NUT-1/PAN)lytic cycle transcript	24	1.3	1.1	1.3	1.4	1.4	4.1	8.9	4.9	3.2	3.2	15	12	15	16	15	46	100	54	36	36
89600-90541	IRF Homolog	24	1.2	1.0	1.3	2.2	2.2	2.6	3.6	5.1	3.5	2.6	24	21	26	44	44	52	70	100	70	51
90173-90643	Herpes glycoprotein X	24	1.1	1.3	1.1	2.1	1.6	2.5	3.9	4.6	3.6	2.8	25	29	25	46	35	54	86	100	80	61

[a] Quantitative information concerning the ratio of expression in BCBL-1 cells following TPA induction compared to that for uninduced cells was extracted from the microarray images and tabulated. Expression was normalized to the maximal expression observed for the gene and color coded according to time of maximal expression. HHV-8 genes are listed according to their physical location on the HHV-8 genome. Viral genes with peak expression at the following times are color coded according to the following scheme: 12 h, pink; 24 h, green; 36 h, red; 48 h, blue; 72 h, maroon; and 96 h, olive. DT represents the time (hours postinduction) at which a doubling in calibrated ratio is seen compared to baseline expression (0 hpi).

tor (Rta) (32) shown to activate the lytic viral cycle (22, 39), has increased expression at 10 hpi. Our data are in accord with studies using Northern blot analyses by Sun et al. (40) which identify these viral ORFs as immediate-early genes expressed 4 to 8 hpi. ORFs involved in DNA replication (32), including ORF 2, encoding dihydrofolate reductase; ORF 6, encoding a DNA binding protein; ORF 9, encoding DNA polymerase; ORFs 56 and 59, which encode DNA replication proteins; ORFs 60 and 61, which encode ribonucleotide reductase; and ORF 62, encoding a protein involved in assembly and DNA maturation, all show increased expression by 10 hpi, indicating preparation for viral DNA replication.

The succeeding subset of genes expressed encodes structural proteins and DNA packaging components (32). Some of the tegument proteins (ORFs 32, 38, 63, and 67) and glycoproteins (ORFs 8, 47, and 68) show relatively early expression at 10 to 12 hpi, while other virion structural genes, including ORFs 17, 25, 26, 65, and 66, which encode capsid proteins; ORFs 19, 64, and 75, which code for tegument proteins; ORFs 29a and 29b, which encode packaging proteins; and ORFs 22, 39, and 48, which encode glycoproteins, first show increased expression somewhat later, at 24 hpi. This differential regulation in expression suggests that certain components may be needed earlier in assembly to optimize virion assembly. The structural genes all peaked in expression levels at 24 to 48 hpi.

HHV-8 has been shown previously to encode a number of proteins that have homology to cellular signaling molecules and immune components (23, 27, 32). Expression of these HHV-8-encoded homologs can be detected throughout the induced lytic cycle, although different cellular homolog genes are expressed with different kinetics. ORF K2, which encodes vIL-6 (25), is among the first viral genes to show increased expression at 8 hpi and peaks in expression level by about 24 hpi. This viral cytokine has been implicated in the pathogenesis of KS. It has been shown to stimulate hematopoiesis and to play a role in angiogenesis through the initiation of vascular endothelial growth factor expression, as well as to stimulate primary effusion lymphoma cells (1, 5, 11, 23). The early expression of vIL-6 reinforces the importance of this cellular homolog in viral infection.

The next set of cellular homologs, with increased expression at 10 hpi, includes the ORF K9-encoded vIRF-1 (32); the ORF 16-encoded vBcl-2 (10); and ORF K1, which can cause cellular transformation (24). Peak levels in expression of these viral homologs are seen between 24 and 48 hpi. These virally encoded gene products may contribute to viral pathogenicity by interfering with the host's intrinsic antiviral mechanisms such as apoptosis (10) and interferon-induced signaling (16), which could hinder viral replication. At 12 hpi, both the ORF K6-encoded chemokine-like protein vMIP-IA and the ORF 74-encoded G-protein-coupled receptor show increased expression and peak in expression by 48 hpi. ORF 4, which encodes a complement binding protein (32), and ORF K12 (kaposin A) (32), which can transform cells (19), do not show increased expression until 24 hpi and do not peak until 48 hpi.

To examine the relationship between the genes and their expression patterns, the data were analyzed using a hierarchical clustering algorithm (14) in which the expression of each gene at every time point was compared and grouped according to the similarity in gene profiles. The data are presented in the form of a colored mosaic matrix where each column represents a time point following induction and every row indicates the expression pattern of a single ORF (Fig. 2). The data are normalized relative to the mean expression level of the ORF

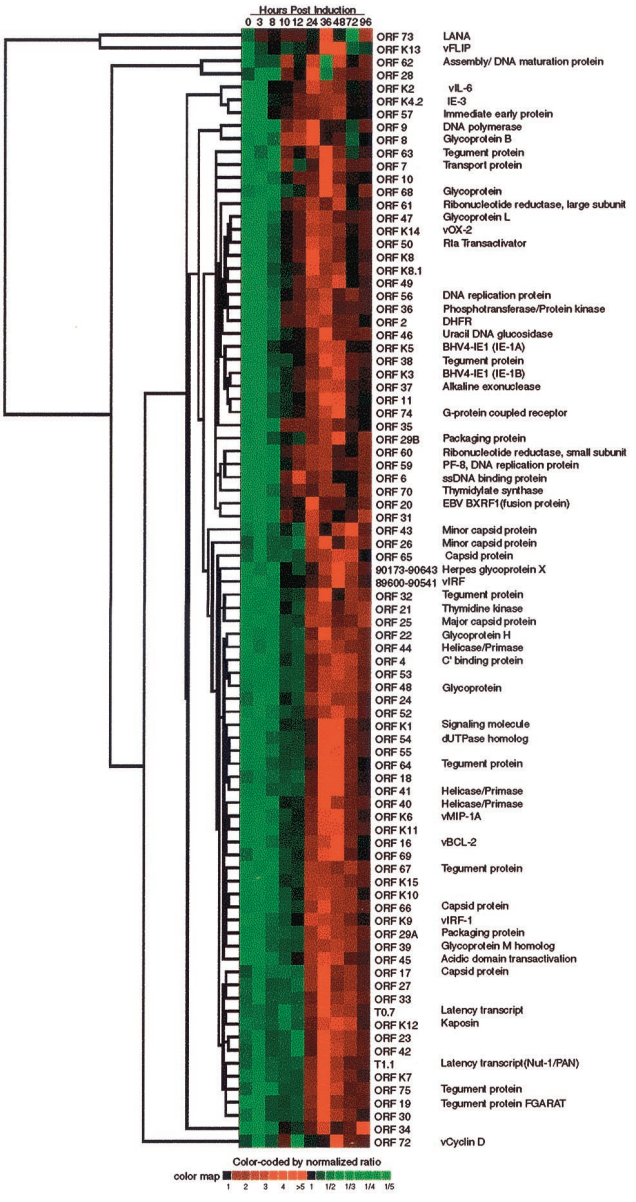

FIG. 2. Hierarchical clustering of HHV-8 gene expression data. Calibrated expression ratios for each gene were cataloged based on the hierarchical clustering program (average-linkage algorithm) in which the temporal expression ratios of genes were compared pairwise and grouped according to their similarity (Pearson's correlation coefficient). Columns indicate separate time points, and every row displays the expression profile of a single ORF. The normalized expression ratios across all the time points are color coded, with green boxes indicating expression ratios lower than the mean and red boxes indicating gene expression greater than the mean. Black boxes indicate an intermediate level of expression. The magnitude of up-regulation from the mean is shown by differing intensities of red, with deep red illustrating lower expression and bright red showing the highest levels of expression. The dendrogram at the left clusters the ORFs based on the relatedness of their gene expression patterns. DHFR, dihydrofolate reductase; BHV4, bovine herpesvirus 4; ssDNA, single-stranded DNA; EBV, Epstein-Barr virus.

divided by the standard deviation of the expression level across all the time points (see Materials and Methods). The normalized expression level of each gene is color coded, with green blocks indicating gene expression ratios lower than the mean and red blocks indicating levels of gene expression higher than the mean. Blocks containing more saturated colors indicate higher levels of expression. Black blocks indicate an intermediate level of expression. The dendrogram at the left of the image assembles all the genes into a single tree with ORFs having related expression patterns joined by a branch. The branch lengths reflect the degree of similarity between the gene expression profiles. Figure 2 illustrates the ordered and varied patterns of viral gene expression. It can be seen that the expression patterns of genes with early expression kinetics are more closely related to one another than to the patterns of those with late expression kinetics. For example, ORF 57, ORF K2, and ORF K4.2, which are expressed early in the lytic cycle, appear clustered together on the top of the table, and genes expressed late in the infection cycle, such as ORF 19 and ORF 75, are found clustered at the bottom of the table, while LANA (ORF 73) and vFLIP (K13/ORF 71), which are constitutively expressed, are distant from both the early regulatory and late structural genes. The clustering display of the data also shows a tendency for genes with similar functions, such as ORFs 26, 43, and 65, which all encode capsid proteins, to be clustered together despite being located apart from one another in the viral genome.

To confirm the microarray results, HHV-8 genes including immediate-early genes ORF K4.2 and ORF 57, early lytic gene ORF 59, and late lytic gene ORF 17 were selected for Northern analysis (Fig. 3). The same PCR-amplified fragments used to construct the arrays were labeled via random priming and hybridized to blots made from the same RNA used in the cDNA synthesis step for the microarrays. The patterns of expression produced by the two assays are similar, and expression peaks at about the same times. This essential agreement between the Northern and array data supports the general applicability and utility of the array approach.

HHV-8 transcription program and physical organization of the genome. Figure 4 shows the expression patterns of the viral genes superimposed on a physical map of the virus (32) to illustrate the relationship between the physical map and the expression data. These data provide a quantitative overview of HHV-8 gene expression during lytic replication. Here, the expression data are normalized to the level of peak expression (set to equal 100) for each gene. The ORFs are color coded by their function, and the graphs are shaded corresponding to the first time point at which a doubling in the calibrated ratio is detected compared to baseline (0 hpi).

The expression patterns of the known genes generally behave as expected: immediate-early genes (e.g., ORF 57 and ORF K5) peak early, while genes encoding virion structural proteins (e.g., ORF 17 and ORF 66) peak later. The map also shows the related patterns of expression for certain genes with common functions. For example, ORFs involved in DNA replication (purple) all show gene expression patterns which rise at 10 hpi (peach) while ORFs encoding helicases-primases (lavender) all show increases in expression at 24 hpi (green). The map clearly illustrates the carefully ordered nature of the viral transcription program.

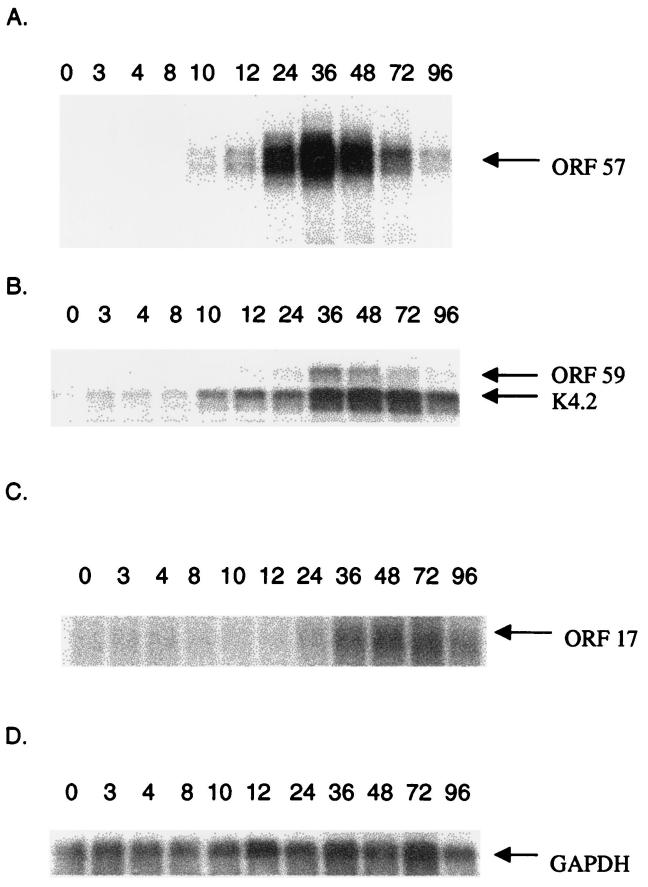

FIG. 3. Northern analyses for HHV-8 genes. HHV-8 genes, ORF 17, ORF 57, ORF 59, and ORF K4.2, were selected for Northern analysis to confirm the results obtained using microarrays. The same PCR-amplified fragments used to construct the arrays were labeled via random priming and hybridized to blots made from the same RNA used in the cDNA synthesis step for microarray assays. Data were collected with a PhosphorImager. The expression patterns obtained using the Northern blots are those expected for the genes, with expression for the immediate-early genes ORF K4.2 and ORF 57 peaking approximately 24 to 48 hpi, that for the early lytic gene ORF 59 peaking at 36 hpi, and that for the late lytic gene ORF 17 peaking at 48 hpi. The data were normalized to account for basal gene expression levels by using uninduced BCBL-1 cells. GAPDH, glyceraldehyde-3-phosphate dehydrogenase.

DISCUSSION

Over 25 years ago, some of the earliest experiments in molecular virology showed that herpesvirus replication proceeds through a strict, temporally ordered transcription program (30, 43). However, the limitations of traditional techniques constrained the ability to determine the quantitative details of herpesvirus transcription programs. Here, we have custom built viral microarrays to provide a comprehensive description of the HHV-8 transcription program and to delineate viral ORFs based on their transcriptional kinetics. The results remarkably echo those initial descriptions, while providing quantitative detail covering the expression patterns of genes with both known and unknown functions and offering insights into viral replication and pathogenesis.

Although the latent infection system of stimulated BCBL-1 cells may not include all the subtle aspects of viral gene ex-

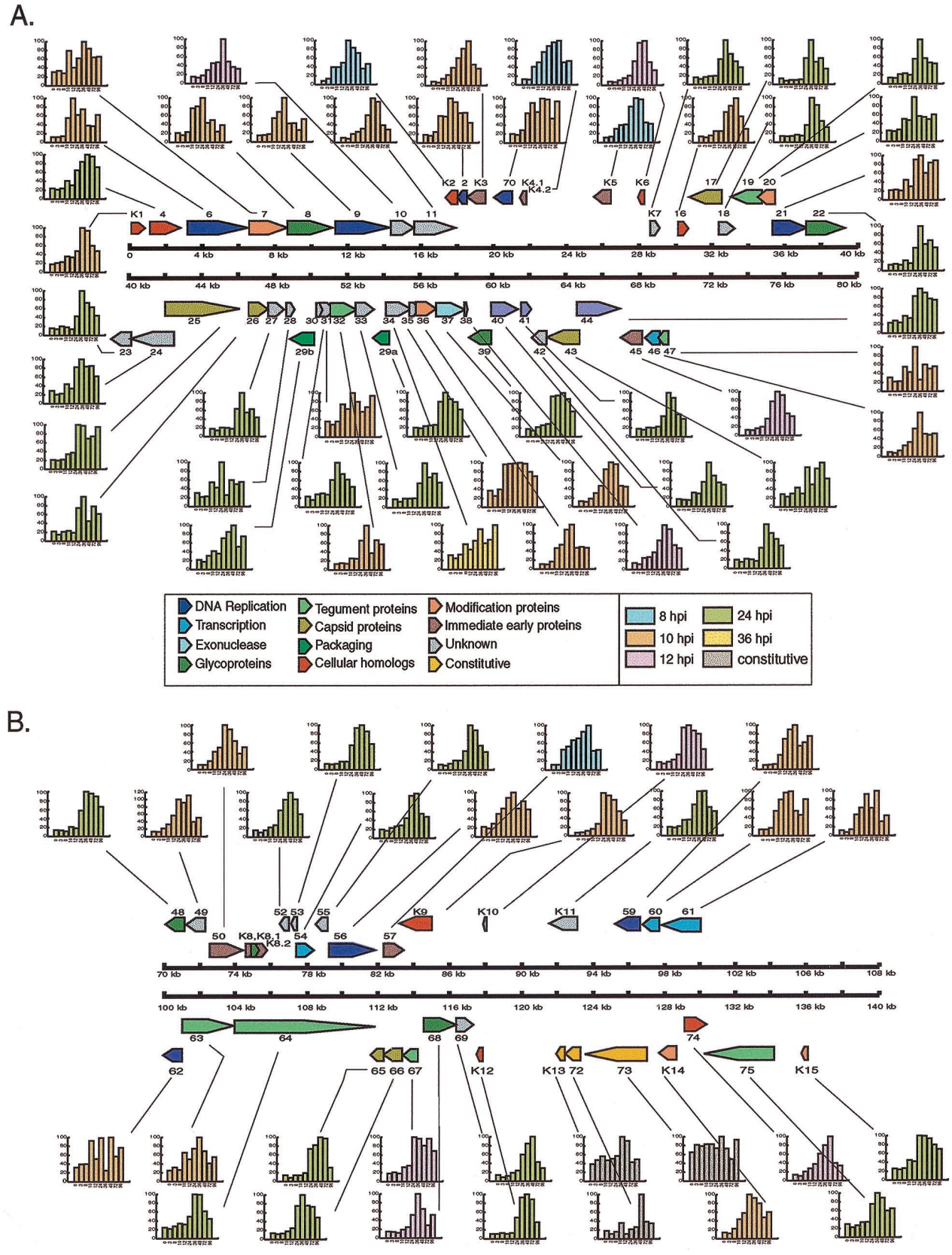

FIG. 4. HHV-8 map. The expression patterns for HHV-8 genes were placed onto a physical map of the virus (32). ORFs are color coded by function. Graphs are shaded by the time at which a doubling in calibrated ratio is seen compared to time 0 hpi (baseline). The expression levels plotted in the graphs are normalized to the maximum expression (set to equal 100) for each gene.

pression evident in more physiologic exogenous infection systems, the patterns of gene expression seen with our microarray analysis concur with the functional roles of the viral genes and agree with published work describing HHV-8 expression kinetics (33, 40). Our results, together with the available data concerning the organization of the HHV-8 genome, permit a viral genome-wide assessment of the interrelationship between genomic structure and the transcription program. Certain ORFs which lie far apart on the genome but which have similar functions display analogous expression patterns. For example, ORFs 25, 43, and 65 encode capsid proteins. Even though they are located apart from one another on the genome, they are late genes expressed with similar patterns and were found to cluster together using the clustering algorithm (Fig. 2). Similarly, ORFs 19, 32, 38, 63, 64, and 75, which encode tegument proteins, are also found in different parts of the genome but are expressed with similar kinetics. It will be interesting to determine whether such genes with similar expression patterns lying far apart on the genome share similar regulatory mechanisms. Conversely, some adjacent genes exhibit quite distinct expression patterns. ORF 56 (DNA replication protein), ORF 57 (immediate-early protein), and ORF K9 (vIRF-1) are located adjacent to one another on the genome but exhibit quite different expression patterns and cluster with other genes of a similar expression class, with ORF 57 showing an immediate-early pattern of expression while the other genes were expressed later (also Fig. 2). Some adjacent genes, such as ORFs 40 and 41, which encode subunits of a helicase-primase and are encoded by a single transcript, show similar patterns of expression, as expected. Other adjacent genes, such as ORFs 65 and 66, which encode capsid proteins, show slightly different patterns, perhaps indicating additional posttranscriptional levels of regulation.

The expression patterns of particular classes of genes obtained in our studies may offer insights into viral replication and pathogenesis strategies. The HHV-8 genome encodes over 80 ORFs, including a large number of cellular gene homologs implicated in pathogenesis (17). As expected, the genes showing the earliest increase in expression are involved in gene regulation. Genes involved in DNA replication show increased expression slightly later, consistent with the classical descriptions of herpesvirus replication programs. Interestingly, the cellular homolog genes are expressed with various kinetics, and these differences in kinetics can offer insights into the role of the cellular homologs in viral replication and pathogenesis strategies. For example, the relatively early expression of vIL-6 (ORF K2) suggests that it may play a particularly important role in optimizing the host or host cell for viral replication.

Following the expression of genes involved in DNA replication, a wave of structural and packaging genes is expressed as the virus shifts to assembly of virions. It is near this time that a second subset of viral homologs is expressed, including genes encoding vBcl-2, vIRF, and a transformation-associated protein (ORF K1 gene product) (19). Apparently, as the structural proteins of the virus are expressed, the virus finds it advantageous to attack the intrinsic host antiviral mechanisms. By activating multiple cellular homologs simultaneously, the virus can potentially prevent programmed cell death of the infected host cell and concurrently alter cell cycle progression. At the end of the lytic cycle, additional viral homologs, including the G-protein-coupled receptor (ORF 74) (2) and kaposin A (ORF K12), involved in cellular transformation (24), are expressed. These genes are apparently required at the end of the viral replication cycle, presumably to optimize the cell for the later stages of the replication cycle.

While many of the HHV-8 ORFs to date remain unclassified, the comprehensive description of the transcription program can serve to suggest functions for these previously uncharacterized genes, since the timing of gene expression is generally related to function. ORFs 11, 31, 35, and 49 are expressed earlier in the induced lytic cycle, at 10 hpi, similar to patterns exhibited by the early transactivators and certain cytokine homologs. ORF 10 shows increased expression at 12 hpi, with an expression pattern similar to those of genes involved in DNA replication. We predict that this gene is involved in the earliest stages of viral replication or in preparing the cell for replication. ORFs K7, 18, 23, 24, 27, 28, 30, 33, 42, 52, 53, and 69 are all expressed later, at 24 hpi, and show patterns of gene expression similar to those for functional classes of structural and packaging proteins and the cellular homologs with late expression patterns. These genes likely encode additional structural components, are involved in virion assembly, or modify the host cell to sustain viral replication, for example, by blunting antiviral functions.

Although arrays can provide a wealth of data concerning gene expression patterns, the approach has some inherent technical limitations. These limitations are particularly apparent when the arrays are used to examine expression patterns of multiply spliced, alternatively spliced, and polycistronic messages. ORF 50, which is expressed as a polycistronic message, encoding ORF K8, ORF K8.1, and ORF K8.2 (35, 44), shows increased expression at 10 hpi, as would be expected for this known immediate-early gene involved in the activation of lytic replication (22, 39). Alternative splicing and transcriptional readthrough events, however, make it difficult with microarray technology to clearly delineate discrete gene expression profiles for the various ORFs within this polycistronic message. The expression patterns that we observed for ORF K8.1 and ORF K8.2 showed no significant differences from that for ORF 50, although it is known that ORF K8.1, which is located downstream of ORF K8, is expressed as a late gene during lytic replication in BCBL-1 cells (21, 46).

ORFs K13 (ORF 71), 72, and 73 have been identified as 3′-coterminal transcripts that are coregulated (12, 41). A 5.4-kb mRNA encodes all three ORFs, while a smaller 1.7-kb bicistronic mRNA has been shown to contain ORF K13 and ORF 72 (12). These ORFs have been classified as latency-associated transcripts, which are not induced by lytic replication. Although our data do indicate constitutive expression levels for ORFs K13/71 (vFLIP), 73 (LANA), and 72 (vCyclin D), an increase in expression of these messages is seen between 36 and 48 hpi for ORF K13/71, at 36 hpi for ORF 73, and at 48 hpi for ORF 72. Interestingly, these time points correspond with the peak expression of many of the virally encoded cellular homologs. Each of these ORFs encodes gene products having activities that affect important aspects of cellular physiology. For example, LANA has been shown to block p53 and pRb and to interfere with apoptosis (15, 28), vCyclin has been associated with cell cycle disruption (20), and vFLIP has been shown previously to inhibit apoptosis (42). These

latent genes, with their distinct activities, may be additionally contributing to the dysfunction caused by the cellular homologs to promote viral infection and disease progression.

Kinetic profiling using viral microarray technology provides a rapid and efficient means to analyze global changes in viral gene expression during infection. Chambers et al. (7) and Stingley et al. (38) have similarly utilized viral arrays to analyze the transcription programs of human cytomegalovirus and herpes simplex virus type 1, respectively. Both studies demonstrate the efficiency of viral arrays in the classification of viral genes based on the kinetics of gene expression. The patterns of HHV-8 gene expression seen here provide insights into the processes of HHV-8 replication and into the manipulation of the host cell by the virus, insights that should improve our understanding of the pathogenesis strategies of the virus and the mechanisms through which it causes disease.

ACKNOWLEDGMENTS

We thank C. Gooden, S. Leighton, T. Pohida, F. Newcomb, and P. Smith for providing assistance in the preparation of viral arrays. We also thank F. Maldarelli and J. Black for providing comments on the manuscript.

This work was supported in part by the NIH Intramural AIDS Targeted Antiviral Program and by the Intramural Research Award from the Division of Clinical Sciences, National Cancer Institute.

REFERENCES

1. **Aoki, Y., E. S. Jaffe, Y. Chang, K. Jones, J. Teruya-Feldstein, P. S. Moore, and G. Tosato.** 1999. Angiogenesis and hematopoiesis induced by Kaposi's sarcoma-associated herpesvirus-encoded interleukin-6. Blood **93:**4034–4043.
2. **Arvanitakis, L., E. Geras-Raaka, A. Varma, M. C. Gershengorn, and E. Cesarman.** 1997. Human herpesvirus KSHV encodes a constitutively active G-protein-coupled receptor linked to cell proliferation. Nature **385:**347–350.
3. **Ausubel, F. M., R. Brent, R. E. Kingston, D. D. Moore, J. G. Seidman, J. A. Smith, and K. Struhl.** 1999. Current protocols in molecular biology. Greene Publishing and Wiley Interscience, New York, N.Y.
4. **Bittner, M., P. Meltzer, Y. Chen, Y. Jiang, E. Seftor, M. Hendrix, M. Radmacher, R. Simon, Z. Yakhini, A. Ben-Dor, N. Sampas, E. Dougherty, E. Wang, F. Marincola, C. Gooden, J. Lueders, A. Glatfelter, P. Pollock, J. Carpten, E. Gillanders, D. Leja, K. Dietrich, C. Beaudry, M. Berens, D. Alberts, and V. Sondak.** 2000. Molecular classification of cutaneous malignant melanoma by gene expression profiling. Nature **406:**536–540.
5. **Boshoff, C., Y. Endo, P. D. Collins, Y. Takeuchi, J. D. Reeves, V. L. Schwieckart, M. A. Siani, T. Sasaki, T. J. Williams, P. W. Gray, P. S. Moore, Y. Chang, and R. A. Weiss.** 1997. Angiogenic and HIV-inhibitory functions of KSHV-encoded chemokines. Science **278:**290–295.
6. **Cesarman, E., Y. Chang, P. S. Moore, J. W. Said, and D. M. Knowles.** 1995. Kaposi's sarcoma-associated herpesvirus-like DNA sequences in AIDS-related body-cavity-based lymphomas. N. Engl. J. Med. **332:**1186–1191.
7. **Chambers, J., A. Angulo, D. Amaratunga, H. Guo, Y. Jiang, J. S. Wan, A. Bittner, K. Frueh, M. R. Jackson, P. A. Peterson, M. G. Erlander, and P. Ghazal.** 1999. DNA microarrays of the complex human cytomegalovirus genome: profiling kinetic class with drug sensitivity of viral gene expression. J. Virol. **73:**5757–5766.
8. **Chang, Y., E. Cesarman, M. S. Pessin, F. Lee, J. Culpepper, D. M. Knowles, and P. S. Moore.** 1994. Identification of herpesvirus-like DNA sequences in AIDS-associated Kaposi's sarcoma. Science **266:**1865–1869.
9. **Chen, Y., E. Dougherty, and M. Bittner.** 1997. Ratio-based decision and quantitative analysis of cDNA microarray images. J. Biomed. Optics **2:**364–374.
10. **Cheng, E. H., J. Nicholas, D. S. Bellows, G. S. Hayward, H. G. Guo, M. S. Reitz, and J. M. Hardwick.** 1997. A Bcl-2 homolog encoded by Kaposi sarcoma-associated virus, human herpesvirus 8, inhibits apoptosis but does not heterodimerize with Bax or Bak. Proc. Natl. Acad. Sci. USA **94:**690–694.
11. **Cohen, T., D. Nahari, L. W. Cerem, G. Neufeld, and B. Z. Levi.** 1996. Interleukin 6 induces the expression of vascular endothelial growth factor. J. Biol. Chem. **271:**736–741.
12. **Dittmer, D., M. Lagunoff, R. Renne, K. Staskus, A. Haase, and D. Ganem.** 1998. A cluster of latently expressed genes in Kaposi's sarcoma-associated herpesvirus. J. Virol. **72:**8309–8315.
13. **Duggan, D. J., M. Bittner, Y. Chen, P. Meltzer, and J. M. Trent.** 1999. Expression profiling using cDNA microarrays. Nat. Genet. **21:**10–14.
14. **Eisen, B. M., P. T. Spellman, P. O. Brown, and D. Botstein.** 1998. Cluster analysis and display of genome-wide expression patterns. Proc. Natl. Acad. Sci. USA **95:**14863–14868.
15. **Friborg, J., W. Kong, M. O. Hottiger, and G. J. Nabel.** 1999. p53 inhibition by the LANA protein of KSHV protects against cell death. Nature **402:**889–894.
16. **Gao, S. J., C. Boshoff, S. Jayachandra, R. A. Weiss, Y. Chang, and P. Moore.** 1997. KSHV ORF K9 (vIRF) is an oncogene which inhibits the interferon signalling pathway. Oncogene **15:**1979–1985.
17. **Haase, A. T.** 1997. Viral gene expression and pathogenesis in three emerging diseases: HIV and AIDS; HTLV-I and HAM/TSP; and HHV-8 and Kaposi's sarcoma. FEMS Immunol. Med. Microbiol. **18:**301–305.
18. **Khan, J., L. H. Saal, M. L. Bittner, Y. Chen, J. M. Trent, and P. S. Meltzer.** 1999. Expression profiling in cancer using cDNA microarrays. Electrophoresis **20:**223–229.
19. **Lee, H., R. Veazey, K. Williams, M. Li, J. Guo, F. Neipel, B. Fleckenstein, A. Lackner, R. C. Desrosiers, and J. U. Jung.** 1998. Deregulation of cell growth by the K1 gene of Kaposi's sarcoma-associated herpesvirus. Nat. Med. **4:**435–440.
20. **Li, M., H. Lee, D. W. Yoon, J. C. Albrecht, B. Fleckenstein, F. Neipel, and J. U. Jung.** 1997. Kaposi's sarcoma-associated herpesvirus encodes a functional cyclin. J. Virol. **71:**1984–1991.
21. **Li, M., J. MacKey, S. C. Czajak, R. C. Desrosiers, A. A. Lackner, and J. U. Jung.** 1999. Identification and characterization of Kaposi's sarcoma-associated herpesvirus K8.1 virion glycoprotein. J. Virol. **73:**1341–1349.
22. **Lukac, D. M., R. Renne, J. R. Kirshner, and D. Ganem.** 1998. Reactivation of Kaposi's sarcoma-associated herpesvirus infection from latency by expression of the ORF 50 transactivator, a homolog of the EBV R protein. Virology **252:**304–312.
23. **Moore, P. S., C. Boshoff, R. A. Weiss, and Y. Chang.** 1996. Molecular mimicry of human cytokine and cytokine response pathway genes by KSHV. Science **274:**1739–1744.
24. **Muralidhar, S., A. M. Pumfery, M. Hassani, M. R. Sadaie, N. Azumi, M. Kishishita, J. Brady, J. Doniger, P. Medveczky, and L. J. Rosenthal.** 1998. Identification of kaposin (open reading frame K12) as a human herpesvirus 8 (Kaposi's sarcoma-associated herpesvirus) transforming gene. J. Virol. **72:**4980–4988.
25. **Neipel, F., J. C. Albrecht, A. Ensser, Y. Q. Huang, J. J. Li, A. E. Friedman-Kien, and B. Fleckenstein.** 1997. Human herpesvirus 8 encodes a homolog of interleukin-6. J. Virol. **71:**839–842.
26. **Nicholas, J., V. Ruvolo, J. Zong, D. Ciufo, H. G. Guo, M. S. Reitz, and G. S. Hayward.** 1997. A single 13-kilobase divergent locus in the Kaposi sarcoma-associated herpesvirus (human herpesvirus 8) genome contains nine open reading frames that are homologous to or related to cellular proteins. J. Virol. **71:**1963–1974.
27. **Nicholas, J., V. R. Ruvolo, W. H. Burns, G. Sandford, X. Wan, D. Ciufo, S. B. Hendrickson, H. G. Guo, G. S. Hayward, and M. S. Reitz.** 1997. Kaposi's sarcoma-associated human herpesvirus-8 encodes homologues of macrophage inflammatory protein-1 and interleukin-6. Nat. Med. **3:**287–292.
28. **Radkov, S. A., P. Kellam, and C. Boshoff.** 2000. The latent nuclear antigen of kaposi sarcoma-associated herpesvirus targets the retinoblastoma-E2F pathway and with the oncogene hras transforms primary rat cells. Nat. Med. **6:**1121–1127.
29. **Renne, R., W. Zhong, B. Herndier, M. McGrath, N. Abbey, D. Kedes, and D. Ganem.** 1996. Lytic growth of Kaposi's sarcoma-associated herpesvirus (human herpesvirus 8) in culture. Nat. Med. **2:**342–346.
30. **Roizman, B., M. Kozak, R. Honess, and G. Hayward.** 1975. Regulation of herpesvirus macromolecular synthesis: evidence for multilevel regulation of herpes simplex 1 RNA and protein synthesis. Cold Spring Harbor Symp. Quant. Biol. **39**(Part 2)**:**687–701.
31. **Roizman, B., and A. Sears.** 1996. Herpes simplex viruses and their replication, p. 2231–2295. *In* B. N. Fields, D. M. Knipe, and P. M. Howley (ed.), Fields virology, 3rd ed., vol. 2. Lippincott-Raven Publishers, Philadelphia, Pa.
32. **Russo, J. J., R. A. Bohenzky, M.-C. Chien, J. Chen, M. Yan, D. Maddalena, J. P. Parry, D. Peruzzi, I. S. Edelman, Y. Chang, and P. S. Moore.** 1996. Nucleotide sequence of the Kaposi sarcoma-associated herpesvirus (HHV8). Proc. Natl. Acad. Sci. USA **93:**14862–14867.
33. **Sarid, R., O. Flore, R. A. Bohenzky, Y. Chang, and P. Moore.** 1998. Transcription mapping of the Kaposi's sarcoma-associated herpesvirus (human herpesvirus 8) genome in a body cavity-based lymphoma cell line (BC-1). J. Virol. **72:**1005–1012.
34. **Schena, M., D. Shalon, R. W. Davis, and P. O. Brown.** 1995. Quantitative monitoring of gene expression patterns with a complementary DNA microarray. Science **270:**467–470.
35. **Seaman, W. T., D. Ye, R. X. Wang, E. E. Hale, M. Weisse, and E. B. Quinlivan.** 1999. Gene expression from the ORF50/K8 region of Kaposi's sarcoma-associated herpesvirus. Virology **263:**436–449.
36. **Shalon, D., S. J. Smith, and P. O. Brown.** 1996. A DNA microarray system for analyzing complex DNA samples using two-color fluorescent probe hybridization. Genome Res. **6:**639–645.
37. **Soulier, J., L. Grollet, E. Oksenhendler, P. Cacoub, D. Cazals-Hatem, P. Babinet, M. F. d'Agay, J. P. Clauvel, M. Raphael, L. Degos, et al.** 1995.

Kaposi's sarcoma-associated herpesvirus-like DNA sequences in multicentric Castleman's disease. Blood **86:**1276–1280.
38. **Stingley, S. W., J. J. Ramirez, S. A. Aguilar, K. Simmen, R. M. Sandri-Goldin, P. Ghazal, and E. K. Wagner.** 2000. Global analysis of herpes simplex virus type 1 transcription using an oligonucleotide-based DNA microarray. J. Virol. **74:**9916–9927.
39. **Sun, R., S. F. Lin, L. Gradoville, Y. Yuan, F. Zhu, and G. Miller.** 1998. A viral gene that activates lytic cycle expression of Kaposi's sarcoma-associated herpesvirus. Proc. Natl. Acad. Sci. USA **95:**10866–10871.
40. **Sun, R., S. F. Lin, K. Staskus, L. Gradoville, E. Grogan, A. Haase, and G. Miller.** 1999. Kinetics of Kaposi's sarcoma-associated herpesvirus gene expression. J. Virol. **73:**2232–2242.
41. **Talbot, S. J., R. A. Weiss, P. Kellam, and C. Boshoff.** 1999. Transcriptional analysis of human herpesvirus-8 open reading frames 71, 72, 73, K14, and 74 in a primary effusion lymphoma cell line. Virology **257:**84–94.
42. **Thome, M., P. Schneider, K. Hofmann, H. Fickenscher, E. Meinl, F. Neipel, C. Mattmann, K. Burns, J. L. Bodmer, M. Schroter, C. Scaffidi, P. H. Krammer, M. E. Peter, and J. Tschopp.** 1997. Viral FLICE-inhibitory proteins (FLIPs) prevent apoptosis induced by death receptors. Nature **386:**517–521.
43. **Wagner, E. K., R. I. Swanstrom, and M. G. Stafford.** 1972. Transcription of the herpes simplex virus genome in human cells. J. Virol. **10:**675–682.
44. **Zhu, F. X., T. Cusano, and Y. Yuan.** 1999. Identification of the immediate-early transcripts of Kaposi's sarcoma-associated herpesvirus. J. Virol. **73:**5556–5567.
45. **Ziegler, J., A. C. Templeton, and G. L. Voegel.** 1984. KS: a comparison of classical, endemic, and epidemic forms. Semin. Oncol. **11:**47–52.
46. **Zoeteweij, J. P., S. T. Eyes, J. M. Orenstein, T. Kawamura, L. Wu, B. Chandran, B. Forghani, and A. Blauvelt.** 1999. Identification and rapid quantification of early- and late-lytic human herpesvirus 8 infection in single cells by flow cytometric analysis: characterization of antiherpesvirus agents. J. Virol. **73:**5894–5902.